



Swansea University
Prifysgol Abertawe



Cronfa - Swansea University Open Access Repository

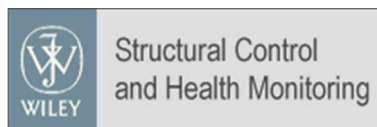
This is an author produced version of a paper published in :
Structural Control and Health Monitoring

Cronfa URL for this paper:
<http://cronfa.swan.ac.uk/Record/cronfa33695>

Paper:

He, D., Wang, X., Friswell, M. & Lin, J. (2017). Identification of modal parameters from noisy transient response signals. *Structural Control and Health Monitoring*, e2019
<http://dx.doi.org/10.1002/stc.2019>

This article is brought to you by Swansea University. Any person downloading material is agreeing to abide by the terms of the repository licence. Authors are personally responsible for adhering to publisher restrictions or conditions. When uploading content they are required to comply with their publisher agreement and the SHERPA RoMEO database to judge whether or not it is copyright safe to add this version of the paper to this repository.
<http://www.swansea.ac.uk/iss/researchsupport/cronfa-support/>



Identification of Modal Parameters from Noisy Transient Response Signals

Journal:	<i>Structural Control and Health Monitoring</i>
Manuscript ID	STC-16-0220.R1
Wiley - Manuscript type:	Research Article
Date Submitted by the Author:	27-Nov-2016
Complete List of Authors:	He, Dan; Xi'an jiaotong university, school of mechanical engineering Wang, Xiufeng; Xi'an jiaotong university, school of mechanical engineering Friskwell, Michael I.; Swansea University, School of Engineering Lin, Jing; Xi'an Jiaotong University, State Key Laboratory for Manufacturing Systems Engineering
Keywords:	Modal identification, Adaptive noise reduction, Low SNR, MMSE-STSA estimator, WIENER-STSA estimator

SCHOLARONE™
Manuscripts

View

1
2
3
4 1 Identification of Modal Parameters from Noisy Transient
5
6 2 Response Signals
7

8 3

9 4

10 5 **Authors:**

11 6

12 7 Dan He, PhD Candidate

13 8 School of Mechanical Engineering

14 9 Xi'an Jiaotong University

15 10 Xi'an, P R China

16 11 Email: hedan0425@stu.xjtu.edu.cn

17 12

18 13 Xiufeng Wang*, PhD, Lecturer

19 14 Shaanxi Key Laboratory of Mechanical Product Quality Assurance and Diagnostics

20 15 Xi'an Jiaotong University

21 16 Xi'an, P R China

22 17 Email: wangxiufeng@mail.xjtu.edu.cn

23 18 Phone number: 86-29-82667938

24 19 Fax: 86-29-83237910

25 20

26 21 Michael I Friswell, PhD, Professor

27 22 College of Engineering

28 23 Swansea University, Bay Campus

29 24 Fabian Way, Crymlyn Burrows

30 25 Swansea SA1 8EN, UK

31 26 Email: m.i.friswell@swansea.ac.uk

32 27

33 28 Jing Lin, PhD, Professor

34 29 State Key Laboratory for Manufacturing Systems Engineering

35 30 Xi'an Jiaotong University

36 31 Xi'an, P R China

37 32 Email: jinglin@mail.xjtu.edu.cn

38 33

39 34

40 35

41 36

42 37

43 38

44 39

45 40

46 41

47
48
49
50
51
52
53
54
55
56
57
58 *Corresponding author

1
2
3 42 Abstract
4
5
6

7
8
9
10
11
12
13
14
15
16
17
18
19
20
21
22
23
24
25
26
27
28
29
30
31
32
33
34
35
36
37
38
39
40
41
42
43
44
45
46
47
48
49
50
51
52
53
54
55
56
57
58
59
60

42 In the process of impact testing of large-scale mechanical equipment, the measured forced
43 response signals are often polluted by strong background noise. The forced response signal has a
44 low signal-to-noise ratio, and this makes it difficult to accurately estimate the modal parameters.
45 To solve this problem, the mean averaging of repeatedly measured frequency response function
46 estimates is often employed in practical applications. However, a large number of impact tests are
47 not practical for the modal testing of large-scale mechanical equipment. The primary objective of
48 this paper is to reduce the number of averaging operations and improve the accuracy of the modal
49 identification by using an adaptive noise removal technique. An adaptive denoising method is
50 proposed by combining the Wiener and improved minimum mean square error short-time spectral
51 amplitude estimators. The proposed method can adaptively remove both stationary and highly
52 non-stationary noise, while preserving the important features of the true forced response signals.
53 The simulation results show that the proposed noise removal technique improves the accuracy of
54 the estimated modal parameters using only one impulse response signal. The experimental results
55 show that the proposed two step method can accurately identify a natural frequency that is very
56 close to a strong interference frequency in the modal test of a 600MW generator casing.

57
58
59
60 KEY WORDS: Modal identification; Adaptive noise reduction; Low SNR; MMSE-STSA
61 estimator; WIENER-STSA estimator
62

1. Introduction

Modal identification estimates the modal model of a structure, i.e. natural frequencies, damping ratios and mode shapes, from measured input-output data. The accuracy of modal identification is highly sensitive to the signal-to-noise ratio (SNR) of the measured output signals(forced response signals). In modal tests of large-scale mechanical equipment, the measured forced response signals are always polluted by strong background noise, and the noise is rather complex as the contributing factors are diverse and complicated. The noise sources are thought to originate from test environment including non-linear effects, extraneous structural noise as well as ‘noise’ in electronic devices[1]. Hence, the forced response signals have a low SNR and this makes the estimation of the modal parameters difficult. To obtain the ideal forced responses the background noise should be removed from the measured forced response signals. Denoising methods have been proposed for noise removal from frequency response functions(FRFs). Kim and Hong [2] proposed a robust wavelet denoising method for FRFs estimation, which is based on a wavelet-related median filtering and wavelet shrinkage to reduce the effect of outliers and zero-mean Gaussian noise respectively. But the method requires many averaging operations for accurate FRF estimation, which reduces the scope of its application. Sanliturk and Cakar [1] presented a method based on the singular value decomposition(SVD) for the elimination of noise from measured FRFs so as to improve the accuracy of modal identification, but the method needs to set an appropriate threshold to avoid loss of valuable information. Alamdari et al. [3] introduced a Gaussian kernel algorithm to reduce unnecessary noise from noisy FRFs, and it is designed to localize damage in the presence of heavy noise influences by using FRFs of the damaged structure only. Huet al. and Bao et al.[4,5] introduced a Cadzow’s algorithm to reduce unnecessary noise from noisy FRFs, but the denoising method needs to set a reasonable noise threshold based on the measured signals. The effectiveness of the denoising methods in [3-5] was illustrated by simulation and experimental data, but none of the results show that the two denoising methods can remove strong background noise mixed in a forced response signal.

Insert Figure 1 here

1
2
3
4 92 Figure 1 shows the basic breakdown of signals into different types[6,7]. The most
5
6 93 fundamental division is into stationary and non-stationary signals. Stationary signals have
7
8 94 statistical properties that are invariant with time, whereas for non-stationary signals the statistical
9
10 95 properties vary with time. Figure 1 highlights that typical measured forced response signals
11
12 96 contain both stationary and non-stationary components for modal tests on large-scale mechanical
13
14 97 equipment. The ideal forced response signal has a transient component that is non-stationary,
15
16 98 background noise that is mainly stationary, and often a continuous component that is
17
18 99 non-stationary. The existing denoising algorithms cannot remove stationary noise and
19
20 100 non-stationary noise simultaneously, and these different types of noise should be dealt with
21
22 101 separately. The short-time spectral amplitude(STSA), Wiener filter(WIENER) and minimum mean
23
24 102 square error(MMSE) methods have been widely used in denoising and coding [8-15]. The
25
26 103 MMSE-STSA estimator is effective in removing stationary signals and the continuous components
27
28 104 of non-stationary signals from measured speech signals[8], although the technique requires the
29
30 105 SNR a priori. Hence this SNR is a key parameter in the MMSE-STSA estimator. The
31
32 106 decision-directed(DD) approach[8] is a widely used method to estimate the a priori SNR, but has
33
34 107 two inherent drawbacks:

- 35 108 • The estimated a priori SNR is biased since the DD approach depends on the estimate of the
36 109 spectrum in the previous [window](#)[8,9].
- 37 110 • The estimated a priori SNR is distorted when the measured signal has a low SNR[8].

38
39 111 The first problem has been solved by an improved a priori SNR estimation method proposed by
40
41 112 Plapouset et al.[9], which removes the bias in the DD approach. However, the second problem is
42
43 113 still unsolved and hence the MMSE-STSA estimator method cannot be directly used to remove
44
45 114 strong background noise mixed in a forced response signal. The Wiener filter is an optimal method
46
47 115 to remove stationary noise in stationary environments[16], whereas the Wiener short-time spectral
48
49 116 amplitude estimator (WIENER-STSA)improves the application scope of the Wiener filter. Here,
50
51 117 the WIENER-STSA estimator can be used to eliminate stationary noise from the measured forced
52
53 118 response signal, so as to solve the second problem. In this paper, we [propose an adaptive](#)
54
55 119 [denoising method](#) combining WIENER-STSA and MMSE-STSA estimators with improved a
56
57 120 priori SNR estimation. The proposed denoising method can adaptively remove stationary noise

1
2
3
4 121 and continuous components of non-stationary noise, while preserving the important features of the
5
6 122 true forced response signals. The proposed method can reduce the number of averaging operations
7
8 123 and improve the accuracy of modal identification for low SNR measurements.

9 124 The paper is organized as follows. Section 2 introduces some background about denoising, and
10
11 125 compares two a priori SNR estimation methods. Section 3 introduces the proposed method. In
12
13 126 section 4, the proposed method is validated using simulated signals. Section 5 applies the
14
15 127 proposed method to measured forced response signals collected from a 600MW generator. Finally,
16
17 128 conclusion are given in Section 6.

18
19 129

20 21 130 2. Background

22 23 131 2.1. The MMSE-STSA estimator

24
25 132 Ephraim and Malah [8] proposed the minimum mean-square error short-time spectral
26
27 133 amplitude(MMSE-STSA) estimator. Previous studies[8, 17] have shown that the MMSE-STSA
28
29 134 estimator has a beneficial effect for the processing of non-stationary signals when the SNR level is
30
31 135 high. [Here the MMSE-STSA developed in \[8\] is reviewed.](#)

32
33 136 In the usual additive noise model, the measured impulse response signal is given by

34
35 137
$$x(t) = s(t) + n(t), \quad 0 \leq t \leq T(1)$$

36
37 138 where $s(t)$ and $n(t)$ denote the noise-free impulse response signal and the noise signal,
38
39 139 respectively, in the analysis interval $[0, T]$. Applying the Short Time Fourier Transform (STFT),
40
41 140 we have

42
43
44 141
$$X_k(p) = S_k(p) + N_k(p) \quad (2)$$

45
46 142 where p and k denote the [short-time window](#) and the frequency indices, respectively. Using
47
48 143 exponential notation, the k -th spectral component of the noise-free impulse response signal and the
49
50 144 noisy signal can be expressed as $S_k(p) = A_k e^{j\alpha_k}$ and $X_k(p) = R_k e^{j\nu_k}$, respectively [8, 9].

51
52 145 The objective of the MMSE-STSA estimator is to determine \hat{A}_k , the estimate of the spectral
53
54 146 amplitude A_k of the noise-free impulse response signals (t) . Ephraim and Malah [8] estimated
55
56 147 \hat{A}_k through the minimization of a Bayesian cost function which measures the mean square error
57
58 148 between \hat{A}_k and A_k . Thus the Bayesian cost function can be expressed as:

$$J = \mathbf{E} \left\{ (A_k - \hat{A}_k)^2 \right\} (3)$$

where $\mathbf{E}\{\cdot\}$ is the expectation operator. The Bayesian estimator is then given by

$$\hat{A}_k = \mathbf{E}\{A_k | x(t), 0 \leq t \leq T\} (4)$$

Assuming the individual spectral components are statistically independent of one another, the expected value of A_k given $\{x(t), 0 \leq t \leq T\}$ is equal to the expected value of A_k given X_k only.

We therefore have

$$\hat{A}_k = \mathbf{E}\{A_k | X_k\} = \frac{\int_0^\infty \int_0^{2\pi} a_k p(X_k | a_k, \alpha_k) p(a_k, \alpha_k) da_k d\alpha_k}{\int_0^\infty \int_0^{2\pi} p(X_k | a_k, \alpha_k) p(a_k, \alpha_k) da_k d\alpha_k} (5)$$

where the symbol a_k denotes the sample value of A_k , and $p(\cdot)$ denotes a probability density function (PDF). In order to develop the theory along the lines that it has been done in the past it is necessary to treat the Discrete Fourier Transform (DFT) coefficients as Gaussian distributions, the assumption is quite poor in some cases but it appears that the resulting algorithm can still provide useful results. With the Gaussian distribution assumption of each individual spectral component of the noise-free impulse response signal and the noisy signal, the conditional PDF of the observed spectral component given a_k and α_k , $p(X_k | a_k, \alpha_k)$, is given by

$$p(X_k | a_k, \alpha_k) = \frac{1}{\pi \lambda_n(k)} \exp \left\{ -\frac{1}{\lambda_n(k)} |X_k - a_k \exp(j\alpha_k)|^2 \right\} (6)$$

and the joint PDF of the impulse response signal spectral amplitude, $p(a_k, \alpha_k)$, is given by

$$p(a_k, \alpha_k) = \frac{a_k}{\pi \lambda_s(k)} \exp \left\{ -\frac{a_k^2}{\lambda_s(k)} \right\} (7)$$

where $\lambda_n(k) \triangleq \mathbf{E}\{|N_k|^2\}$ and $\lambda_s(k) \triangleq \mathbf{E}\{|S_k|^2\}$ are the variance of the k -th spectral component of the noisy signal and the noise-free impulse response signal, respectively. Substituting Eqs. (6) and (7) into Eq. (5), the MMSE-STSA estimator of the impulse response signal spectral amplitude is obtained as

$$\hat{A}_k = \sqrt{\left[\frac{1}{\lambda_s(k)} + \frac{1}{\lambda_n(k)} \right]^{-1}} \cdot \Gamma(1.5) \cdot M \left(-0.5; 1; -\frac{SNR_{prior}(k)}{1 + SNR_{prior}(k)} SNR_{post}(k) \right) \cdot A_k (8)$$

where $\Gamma(\cdot)$ is the gamma function, with $\Gamma(1.5) = \frac{\sqrt{\pi}}{2}$, $M(a; b; c)$ is the confluent hypergeometric function, and $SNR_{prior}(k)$ and $SNR_{post}(k)$ represent the a priori Signal-to-Noise Ratio (SNR) and the a posteriori SNR, respectively. $SNR_{prior}(k)$ and $SNR_{post}(k)$ are defined by

$$174 \quad SNR_{post}(k) = \frac{|X_k|^2}{E\{|N_k|^2\}} \quad (9)$$

$$175 \quad SNR_{prior}(k) = \frac{E\{|S_k|^2\}}{E\{|N_k|^2\}} \quad (10)$$

176 Finally, applying the inverse STFT operation and the phase information of the measured
 177 signal, the estimator of the noise-free impulse response signal can be obtained. In practical
 178 implementations of the MMSE-STSA estimator, $E\{|S_k|^2\}$ and $E\{|N_k|^2\}$ are unknown since only
 179 the measured signal spectrum X_k is available. Thus, both $E\{|S_k|^2\}$ and $E\{|N_k|^2\}$ have to be
 180 estimated. In practice, $E\{|N_k|^2\}$ can be easily estimated during pauses in the impulse response using
 181 a classic recursive relation [17], continuously using Minimum Statistics [18] or Minima
 182 Controlled Recursive Averaging [19], whereas the priori SNR is a key parameter in the
 183 MMSE-STSA estimator. The estimation of the priori SNR will be discussed in detail in the
 184 following sections.

186 2.2. The a priori SNR estimation method

187 A widely used method to determine the a priori SNR from distorted speech is the
 188 decision-directed (DD) approach. Ephraim and Malah [8] defined the DD approach as a linear
 189 combination of the a posteriori SNR and the instantaneous SNR, with a weighting parameter, β ,
 190 that is constrained to be $0 < \beta < 1$. The linear combination gives

$$191 \quad S\hat{N}R_{prior}^{DD}(p, k) = \beta \frac{|\hat{s}^{(p-1,k)}|^2}{\hat{\gamma}_n(p,k)} + (1 - \beta) P[S\hat{N}R_{post}(p, k) - 1] \quad (11)$$

192 where p and k denote the [short-time window](#) and frequency indices, respectively, $P[x] = x$ if
 193 $x \geq 0$ and $P[x] = 0$ otherwise. The parameter β is set to a typical value of 0.98 for the DD
 194 approach. However, Plapous et al. [9] showed that the DD algorithm introduces a [window delay](#)
 195 when the parameter β is close to one, and this delay introduces a bias in the SNR estimation.
 196 Consequently, the DD algorithm computed at the current window p matches that at the previous
 197 [window](#) $p - 1$. Thus, Plapous et al. [9] proposed to compute the SNR for the next [window](#) $p + 1$
 198 using the DD approach and to apply it to the current [window](#) because of the [window delay](#). Hence,
 199 an improved a priori SNR estimation method is

$$200 \quad S\hat{N}R_{prior}^{TSNR}(p, k) = \beta \frac{|G_{mmse}^{DD}(p,k)X(p,k)|^2}{\hat{\gamma}_n(p,k)} + (1 - \beta) P[S\hat{N}R_{post}(p + 1, k) - 1] \quad (12)$$

1
2
3 201 The improved a priori SNR estimation method solves the bias problem while maintaining the
4
5 202 benefits of the DD approach [9]. In order to measure the performance of SNR estimators, it is
6
7 203 useful to compare the estimated SNR values to the true(actual) ones, as shown in Figure 2 where
8
9 204 the estimated SNRs are displayed versus the true SNRs. The SNRs are plotted for a simulated
10
11 205 signal(to be described in detail in Section 4) to focus the analysis on the behavior of the SNR
12
13 206 estimators for forced response components.

14
15 207
16
17 208 Insert Figure 2 here
18
19 209

20
21 210 Figure 2 compares the actual SNR versus the estimated SNRs using the posteriori algorithm,
22
23 211 the improved algorithm and the DD algorithm given by Eqs.(9), (11) and (12), respectively. In this
24
25 212 case, the solid line corresponds to the actual SNR that can be used as a reference. From Figure 2, it
26
27 213 is obvious that the a priori SNR estimator based on the improved algorithm is closer to the actual
28
29 214 SNR than the a priori SNR estimator based on the DD algorithm at higher SNR levels. However,
30
31 215 the a priori SNR estimator based on the improved algorithm departs from the true SNR at lower
32
33 216 SNR levels. The improved algorithm is superior to the traditional DD algorithm when the
34
35 217 measured impulse response signal has a higher SNR, but is distorted when the measured impulse
36
37 218 response signal has a low SNR. In order to avoid the low SNR situation, the WIENER-STSA
38
39 219 estimator will be introduced to improve the SNR.

40 41 221 **2.3 The WIENER-STSA estimator**

42
43 222 The Wiener filter is an optimal method to remove stationary noise in stationary environments
44
45 223 [16]. Here, the WIENER-STSA estimator is introduced to enhance the application scope of the
46
47 224 Wiener filter. Adopting the noise model mentioned in Section2.1, we assume $s(t)$ and $n(t)$ to
48
49 225 be uncorrelated stationary random process, with power spectral density functions denoted by
50
51 226 $S_s(k)$ and $S_n(k)$ respectively, where k denotes the frequency index. One approach to recover the
52
53 227 desired signals(t) relies on the additivity of power spectra

54
55 228
$$S_x(k) = S_s(k) + S_n(k)(13)$$

56
57 229 To recover a sequence $s(t)$ corrupted by additive noise $n(t)$, that is from the sequence

230 $x(t) = s(t) + n(t)$, a linear filter $h(t)$ is found, such that the sequence $\hat{s}(t) = h(t) * x(t)$
 231 minimizes the expected value of the noise, under the condition that the signals $s(t)$ and $n(t)$ are
 232 stationary and uncorrelated. The frequency domain solution to this stochastic optimization
 233 problem is given by

$$234 \quad H(k) = \frac{S_s(k)}{S_s(k) + S_n(k)} \quad (14)$$

235 which is referred as the Wiener filter. Since the Wiener filter is derived under uncorrelated and
 236 stationary conditions, the Wiener filter provides noise suppression without significant distortion in
 237 the estimated signal and the background residual. The STFT is applied when the background and
 238 desired signals are non-stationary, and then $S_s(k)$ and $S_n(k)$ can be expressed as time varying
 239 functions $S_s(p, k)$ and $S_n(p, k)$, where p represents the short-time window. Thus every time
 240 window is processed by a different Wiener filter, defined as

$$241 \quad H(p, k) = \frac{\hat{S}_s(p, k)}{\hat{S}_s(p, k) + \hat{S}_n(p, k)} = \frac{\frac{\hat{S}_s(p, k)}{\hat{S}_n(p, k)}}{1 + \frac{\hat{S}_s(p, k)}{\hat{S}_n(p, k)}} = \frac{\text{SNR}(p, k)}{1 + \text{SNR}(p, k)} \quad (15)$$

242 The reduction of the noise is based on obtaining an accurate SNR [20]. In order to effectively
 243 remove stationary noise, an instantaneous SNR will be introduced, defined as

$$244 \quad \text{SNR}_{inst}(p, k) = \frac{|X(p, k)|^2 - E[|N(p, k)|^2]}{E[|N(p, k)|^2]} \quad (16)$$

245 where $X(p, k)$ is available, and the estimators of $E[|N(p, k)|^2]$ have been introduced in Section
 246 2.1. Hence, the WIENER-STSA estimator is obtained as

$$247 \quad \hat{S}(p, k) = H(p, k) \cdot X(p, k) = \frac{\text{SNR}_{inst}(p, k)}{1 + \text{SNR}_{inst}(p, k)} \cdot X(p, k). \quad (17)$$

248 Finally, applying the inverse STFT operation and the phase information of the measured signal,
 249 the estimator of the noise-free impulse response signal can be obtained.

250

251 3. Proposed Method

252 We assume that the ideal forced response signal is the transient component of non-stationary
 253 signal, and the background noise has a stationary component and a continuous component that is
 254 non-stationary. An adaptive denoising method is proposed to obtain the ideal forced response

1
2
3
4 255 signal. In the first step, the WIENER-STSA estimator is used to remove the stationary signal
5
6 256 components, which is very helpful in improving the SNR of the measured forced response signals
7
8 257 and make the filtered signals suitable for further processing. In the second step, the MMSE-STSA
9
10 258 estimator with an improved a priori SNR estimation method is introduced, which can be used to
11
12 259 remove the continuous component of the non-stationary signal. The flow chart of the proposed
13
14 260 method is shown in Figure 3.

15 261

16
17 262 Insert Figure 3 here

18
19 263

20
21 264 The implementation of the proposed denoising method is summarized below:

22
23 265 (1) Estimate the noise PSD $E[|N(p, k)|^2]$ during no forced response using the Minima
24
25 266 Controlled Recursive Averaging approach [19].

26
27 267 (2) Calculate the instantaneous SNR using Eq. (16).

28
29 268 (3) Remove stationary noise components from the measured forced response signal using the
30
31 269 WIENER-STSA estimator with an instantaneous SNR estimation method.

32
33 270 (4) Re-estimate the noise PSD $E[|N(p, k)|^2]$ during no forced response using the Minima
34
35 271 Controlled Recursive Averaging approach [19].

36
37 272 (5) Calculate the improved a priori SNR using Eq. (12).

38
39 273 (6) Remove residual non-stationary noise from the filtered forced response signals using the
40
41 274 MMSE-STSA estimator with the improved a priori SNR estimation method.

42
43 275

44
45 276 In this paper, the a priori SNR estimation always uses the improved a priori SNR estimation
46
47 277 method, and the following parameters have been chosen: short-time window $p = 0.06s$, windows
48
49 278 overlap 50% and weighting parameter $\beta=0.98$.

50
51 279

52 53 280 4. Simulated Example

54
55 281 To validate the proposed method, a simulated signal, $x(t)$, is generated according to the
56
57 282 model

$$\begin{aligned}
 x(t) = \sum_{i=7} \left(s_1 \cdot e^{-\zeta_1(t-i)} \cdot \cos(2\pi f_{n1}(t-i)) + s_2 \cdot e^{-\zeta_2(t-i)} \cdot \cos(2\pi f_{n2}(t-i)) \right) \\
 + \left(s_3 \cdot e^{-\zeta_3(t-i)} \cdot \cos(2\pi f_{n3}(t-i)) + s_4 \cdot e^{-\zeta_4(t-i)} \cdot \cos(2\pi f_{n4}(t-i)) \right) \\
 + \left((s_5 \cdot \cos(2\pi f_{r1}t)) \cdot (s_6 \cdot \cos(2\pi f_{r2}t) + s_7 \cdot \cos(2\pi f_{r3}t) + 1) \right) \cdot \text{random noise} \quad (14)
 \end{aligned}$$

284 The parameters of the simulated signal are given in Tables 1 and 2, and the sampling frequency is
285 1024Hz.

286

287 Insert Table 1 here

288 Insert Table 2 here

289

290 The simulated signal, $x(t)$, is composed of two terms. The first term represents a forced
291 response signal, where s_1 , s_2 , s_3 and s_4 are the amplitudes of the impulse response signal, f_{n1} ,
292 f_{n2} , f_{n3} and f_{n4} are the corresponding natural frequencies and i is the sample time increment.

293 The second term represents noise components. According to the mathematical model and the
294 parameters the simulated signal has the following three characteristics.

- 295 (1) The forced response signal has a low SNR(SNR=-4.6dB).
- 296 (2) The noise components contain stationary noise and non-stationary noise.
- 297 (3) The noise components contain a base frequency(f_{r1}), which is very close to a natural
298 frequency(f_{n2}) and makes it difficult to accurately estimate the natural frequency(f_{n2}).

299

300 The simulated signal $x(t)$ is shown in Figure 4; the simulated signal contains significant
301 environmental noise, and the forced response signal has a low SNR. The proposed denoising
302 method was applied to the simulated signal, and the results are shown in Figure 5 and Figure 6.
303 Figure 5 compares the filtered signals from the MMSE-STSA and the proposed methods in the
304 time domain, and Figure 6 compares the results in the frequency domain. Figure 6 shows that the
305 natural frequencies cannot be accurately estimated using the raw simulated forced response signal
306 spectrum.

307

308 Insert Figure 4 here

309 Insert Figure 5 here

310 Insert Figure 6 here

1
2
3 311
4
5 312 Figure 5 shows that both the MMSE-STSA and the proposed method can remove most of the
6
7 313 environmental noise. The zoomed part of Figure 5 shows that the filtered signal with only the
8
9 314 MMSE-STSA method is distorted in the time domain. According to the simulated signal
10
11 315 parameters, the first two true natural frequencies are 44.0Hz and 50.0Hz; however Figure 6 shows
12
13 316 that the filtered first two natural frequencies using the MMSE-STSA method are predicted to be
14
15 317 42.0Hz and 49.5Hz. Figure 5 and Figure 6 show that the filtered signal with the proposed method
16
17 318 has a good consistency with the ideal forced response signal in both the time and frequency
18
19 319 domains. Meanwhile, the strong colored noise frequency(49.5Hz) disappears after the filter
20
21 320 operation of the proposed method, and the two close natural frequencies (44.0Hz, 50.0Hz) are
22
23 321 accurately estimated. The simulation results indicates that using the WIENER-STSA estimator
24
25 322 before the MMSE-STSA estimator under low SNR conditions significantly improves the
26
27 323 estimation. The proposed noise removal technique can improve the accuracy of the estimated
28
29 324 modal parameters using only one impulse response signal in a strong background noise
30
31 325 environment.
32
33 326

34 327 5. Experiment Results from a 600MW Generator

36 328 5.1. Experimental setup

37
38 329 In this section, the proposed method is validated using the measured forced response signals
39
40 330 collected from a 600MW generator. The generator exhibits excessive vibration during operation,
41
42 331 and the rotating frequency of the generator is 50Hz. Figure 7 shows the image of the generator,
43
44 332 and the generator shell located inside a sound-proof housing. Figure 8 shows the bode diagram of
45
46 333 the generator; the generator has a resonance frequency at 48.5Hz, which is not the natural
47
48 334 frequency of the rotor according to the simulated results. Hence, this resonance frequency is likely
49
50 335 to be a natural frequency of the generator shell. A modal test was performed to obtain the natural
51
52 336 frequencies of the generator shell. However, the measured forced response signal is polluted by
53
54 337 highly non-stationary noise, and the measured forced response signal has a low SNR. The spectral
55
56 338 analysis of the measured signal shows that the forced response signal contains a strong colored
57
58 339 noise; the strong colored noise frequency is 49.8Hz, which is very close to the resonance
59
60

1
2
3 340 frequency at 48.5Hz. This makes it difficult to accurately estimate the natural frequency of the
4
5 341 generator shell. It should be mentioned that the state-of-the-art method (PolyMAX algorithm)
6
7 342 estimates the natural frequency to be 49.8Hz, which indicates that the strong colored noise signal
8
9 343 has a great influence on modal parameter identification.

10 344

11 345 Insert Figure 7 here

12 346 Insert Figure 8 here

13 347

14 348 **5.2. Experimental results**

15 349 The time domain waveform of the measured signal is shown in Figure 9. The measured signal
16 350 contains high levels of environmental noise, and the forced response signal has a low SNR. The
17 351 proposed denoising method was applied to the measured forced response signal, and the results
18 352 are shown in the time and frequency domains in Figure 10 and Figure 11 respectively. The filtered
19 353 signal from the MMSE-STSA and the proposed methods are compared. Figure 11 shows that the
20 354 natural frequencies cannot be accurately estimated from the raw measured forced response signal
21 355 spectrum. Figure 10 shows that most of the environmental noise has been removed by both the
22 356 MMSE-STSA and proposed methods. Figure 11 shows that the colored noise frequency (49.8Hz)
23 357 has been filtered using both the MMSE-STSA method and the proposed method, but a natural
24 358 frequency close to the interference frequency (49.8Hz) disappears with the MMSE-STSA method.
25 359 This demonstrates that the MMSE-STSA method may lead to distortion of the estimated modal
26 360 parameters in noisy environments. In contrast, Figure 11 shows that a natural frequency at 48.9Hz
27 361 appears after using the proposed method, and the result is consistent with the Bode diagram during
28 362 the rotor startup. Thus, the application of the WIENER-STSA estimator is necessary before the
29 363 MMSE-STSA estimator under low SNR conditions, and the proposed method can help to
30 364 accurately identify natural frequencies in modal tests of large-scale mechanical equipment.

31 365

32 366 Insert Figure 9 here

33 367 Insert Figure 10 here

34 368 Insert Figure 11 here

35 369

370 6. Conclusion

371 In this paper, we focus on modal parameter identification when the forced response signal has a
372 low SNR. [An adaptive denoising method](#) based on the WIENER-STSA estimator and an improved
373 MMSE-STSA estimator was proposed. Comparing the proposed method with some
374 state-of-the-art denoising methods in Ref. [1,2], the proposed method does not need to set an
375 appropriate threshold to avoid loss of valuable information, and does not require many averaging
376 operations. The proposed method can adaptively remove stationary and non-stationary noise
377 components, while preserving the important features of the true forced response signals. The
378 simulation shows that the proposed noise removal technique improves the accuracy of the
379 estimated modal parameters using only one impulse response signal, which demonstrates that the
380 proposed method can reduce the number of averaging operations when the measured forced
381 response signal has a low SNR. In the modal test of a 600MW generator shell, the measurement
382 results show that, in contrast to the state-of-the-art method (PolyMAX algorithm), the proposed
383 method can accurately identify a natural frequency that is very close to a strong interference
384 frequency. Consequently, [the proposed adaptive method](#) is a powerful tool to improve the accuracy
385 of modal identification when the forced response signal has a low SNR.

386

387 7. Acknowledgement

388 The work is supported by Natural Science Foundation of China (Nos. 51421004), and the
389 High-end CNC machine tools and fundamental manufacturing equipment key state science and
390 technology projects (Grant No. 2012ZX04012032).

391

392

393 References

- 394 1. Sanliturk KY, Cakar O: Noise elimination from measured frequency response functions.
395 *Mechanical Systems & Signal Processing* 2005; **19**(3):615-631,
396 DOI:10.1016/j.ymssp.2004.04.005.
- 397 2. Kim YY, Hong JC, Lee NY. Frequency Response Function Estimation via a Robust Wavelet
398 DeNoising Method. *Journal of Sound & Vibration* 2001; **244**(4):635-649,
399 DOI:10.1006/jsvi.2000.3509.
- 400 3. Alamdari MM, Li J, Samali B: FRF-based damage localization method with noise
401 suppression approach. *Journal of Sound & Vibration* 2014, **333**(14):3305-3320,
402 DOI:10.1016/j.jsv.2014.02.035.
- 403 4. Hu SLJ, Bao X, Li H: Model order determination and noise removal for modal parameter
404 estimation. *Mechanical Systems & Signal Processing* 2010, **24**(6):1605-1620,
405 DOI:10.1016/j.ymssp.2010.01.005.
- 406 5. Bao XX, Li CL, Xiong CB: Noise elimination algorithm for modal analysis. *Applied Physics*
407 *Letters* 2015, **107**(4):3777.DOI: 10.1063/1.4927642.
- 408 6. Randall RB: Noise and vibration data analysis. *Handbook of Noise and Vibration Control*
409 2007:549-564. DOI: 10.1002/9780470209707.ch46.
- 410 7. Randall RB: *Vibration-based condition monitoring: industrial, aerospace and automotive*
411 *applications*: John Wiley & Sons; 2011. DOI: 10.1002/9780470977668.
- 412 8. Ephraim Y, Malah D: Speech enhancement using a minimum-mean square error short-time
413 spectral amplitude estimator. *IEEE Transactions on Acoustics Speech & Signal Processing* 1984,
414 **32**(6):1109-1121.DOI: 10.1109/TASSP.1984.1164453.
- 415 9. Plapous C, Marro C, Scalart P: Improved Signal-to-Noise Ratio Estimation for Speech
416 Enhancement. *Audio Speech & Language Processing IEEE Transactions on* 2006,
417 **14**(6):2098-2108.DOI: 10.1109/TASL.2006.872621.
- 418 10. Imsiya KA, Nandana BT: Speech source separation and noise reduction using a MMSE
419 short-time spectral amplitude estimator. In *Innovations in Information, Embedded and*
420 *Communication Systems (ICIECS), 2015 International Conference on: 2015*; 2015.DOI:
421 10.1109/ICIECS.2015.7193178.
- 422 11. Abutalebi HR, Rashidinejad M: Speech enhancement based on β -order MMSE estimation of
423 Short Time Spectral Amplitude and Laplacian speech modeling. *Speech Communication* 2015,
424 **67**:92-101.DOI: 10.1016/j.specom.2014.12.002.
- 425 12. Djouama A, Lim MS, Ettoumi FY: Erratum to: Channel Estimation in Long Term Evolution
426 Uplink Using Minimum Mean Square Error-Support Vector Regression. *Wireless Personal*
427 *Communications* 2015, **80**(1):447-447. DOI:10.1007/s11277-014-2191-3.
- 428 13. Sudeep PV, Palanisamy P, Kesavadas C, Rajan J: Nonlocal linear minimum mean square
429 error methods for denoising MRI. *Biomedical Signal Processing & Control* 2015, **20**:125-134.
430 DOI: 10.1016/j.bspc.2015.04.015.
- 431 14. Tiwari M, Gupta B: Image Denoising using Spatial Gradient Based Bilateral Filter and
432 Minimum Mean Square Error Filtering. *Procedia Computer Science* 2015,
433 **54**:638-645.DOI:10.1016/j.procs.2015.06.074.
- 434 15. Drouet J, Leclère Q, Parizet E: Experimental modeling of Wiener filters estimated on an
435 operating diesel engine. *Mechanical Systems & Signal Processing* 2015, s 50-51:646-658.DOI:

- 1
2
3 436 10.1016/j.ymsp.2014.05.027.
4 437 16. Lim JS, Oppenheim AV: Enhancement and bandwidth compression of noisy speech.
5 438 *Proceedings of the IEEE* 1980, **67**(12):1586-1604.DOI: 10.1109/PROC.1979.11540.
6
7 439 17. Scalart P, Filho JV: Speech enhancement based on a priori signal to noise estimation. In
8 440 *Acoustics, Speech, and Signal Processing, IEEE International Conference on: 1996*;
9 441 **1996**:629-632.DOI: 10.1109/ICASSP.1996.543199.
10 442 18. Martin R: Noise power spectral density estimation based on optimal smoothing and minimum
11 443 statistics. *Speech & Audio Processing IEEE Transactions on* 2001, **9**(5):504-512.DOI:
12 444 10.1109/89.928915.
13 445 19. Cohen I, Berdugo B: Noise estimation by minima controlled recursive averaging for robust
14 446 speech enhancement. *Signal Processing Letters IEEE* 2002, **9**(1):12-15.DOI: 10.1109/97.988717.
15 447 20. El-Fattah MAA, Dessouky MI, Abbas AM, Diab SM, El-Rabaie ESM, Al-Nuaimy W,
16 448 Alshebeili SA, El-Samie FEA: Speech enhancement with an adaptive Wiener filter. *International*
17 449 *Journal of Speech Technology* 2014, **17**(1):53-64. DOI: 10.1007/s10772-013-9205-5.
18
19 450
20
21 451
22
23
24
25
26
27
28
29
30
31
32
33
34
35
36
37
38
39
40
41
42
43
44
45
46
47
48
49
50
51
52
53
54
55
56
57
58
59
60

1
2
3
4
5
6
7
8
9
10
11
12
13
14
15
16
17
18
19
20
21
22
23
24
25
26
27
28
29
30
31
32
33
34
35
36
37
38
39
40
41
42
43
44
45
46
47
48
49
50
51
52
53
54
55
56
57
58
59
60

452 Table list

453

Table 1. The frequencies of the simulated signal

f_{n1} (Hz)	f_{n2} (Hz)	f_{n3} (Hz)	f_{n4} (Hz)	f_{r1} (Hz)
44.0	50.0	65.0	80.0	49.5

454

455

Table 2. The parameters of the simulated signal

s_1	s_2	s_3	s_4	s_5	s_6	s_7	ζ_1	ζ_2	$T(s)$
8.00	14.00	12.00	13.00	5.90	0.13	0.16	10	6	6.3

456

457

For Peer Review

1
2
3
4 458 Figure list
5

6 459 Figure 1. Classification of signals.
7

8
9 460 Figure 2. The actual and estimated SNRs for a simulated signal.
10

11 461 Figure 3. Flow chart of the proposed method.
12

13 462 Figure 4. Time domain waveforms of the simulated signal.
14

15
16 463 Figure 5. The simulated signal waveform before and after filtering.
17

18
19 464 Figure 6. The simulated signal spectrum before and after filtering.
20

21 465 Figure 7 The image of the generator: (a) Generator and sound-proof housing, (b) Generator shell
22

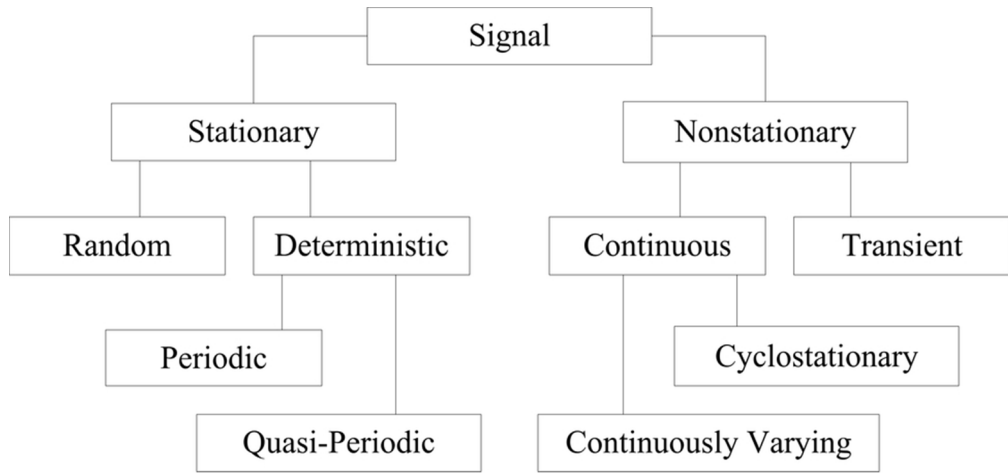
23
24 466 Figure 8. Bode diagram of the rotor response during startup.
25

26 467 Figure 9. Time domain waveforms of the measured signal.
27

28
29 468 Figure 10. The measured signal waveform before and after filtering.
30

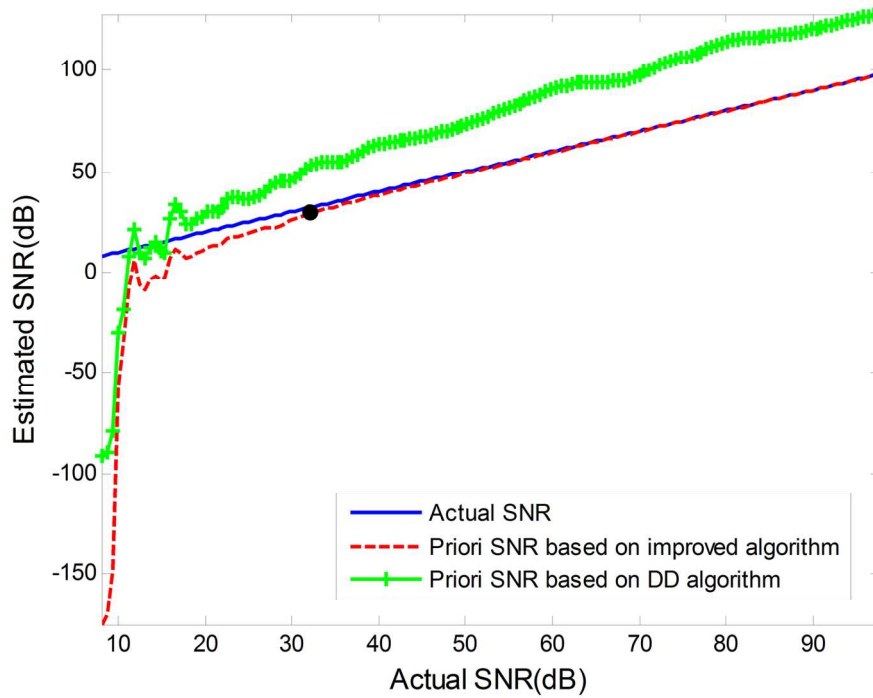
31 469 Figure 11. The measured signal spectra before and after filtering.
32
33
34
35
36
37
38
39
40
41
42
43
44
45
46
47
48
49
50
51
52
53
54
55
56
57
58
59
60

1
2
3
4
5
6
7
8
9
10
11
12
13
14
15
16
17
18
19
20
21
22
23
24
25
26
27
28
29
30
31
32
33
34
35
36
37
38
39
40
41
42
43
44
45
46
47
48
49
50
51
52
53
54
55
56
57
58
59
60



82x38mm (300 x 300 DPI)

Peer Review

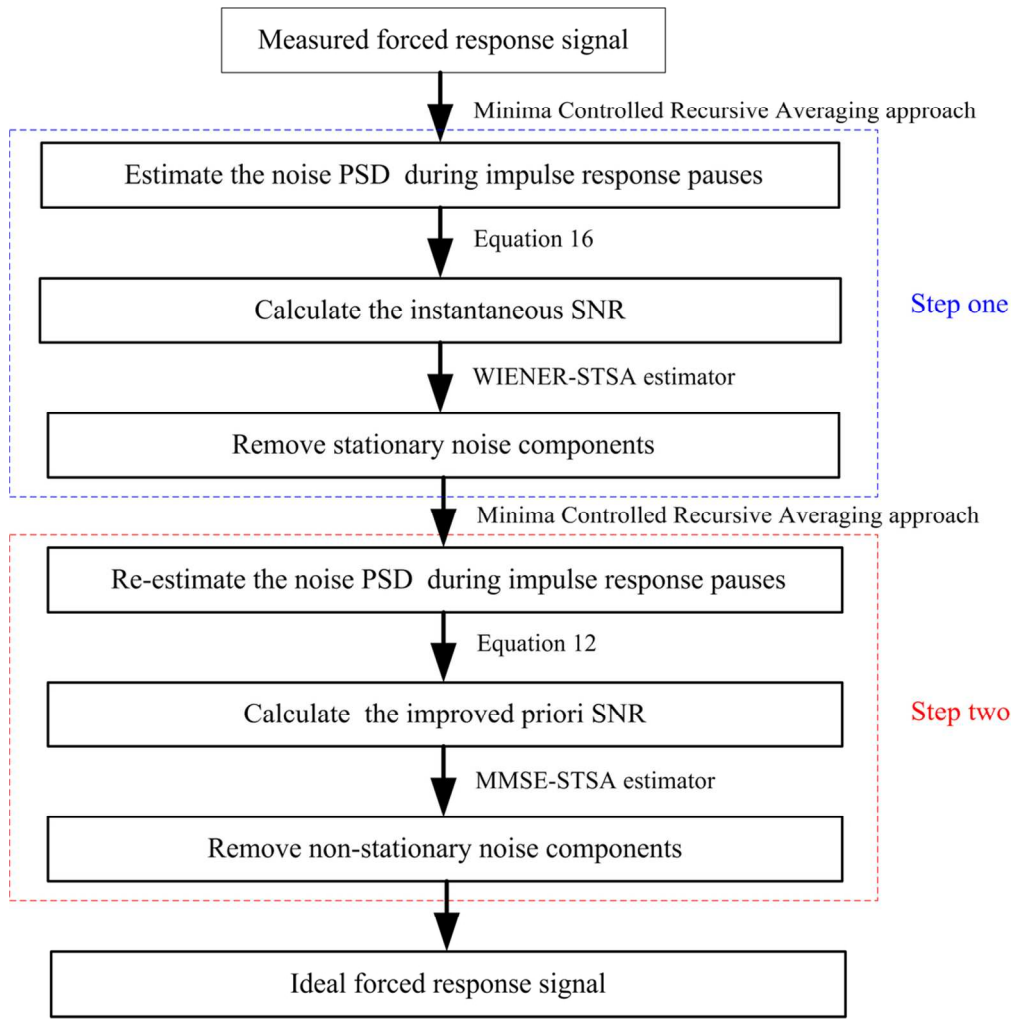


148x111mm (300 x 300 DPI)

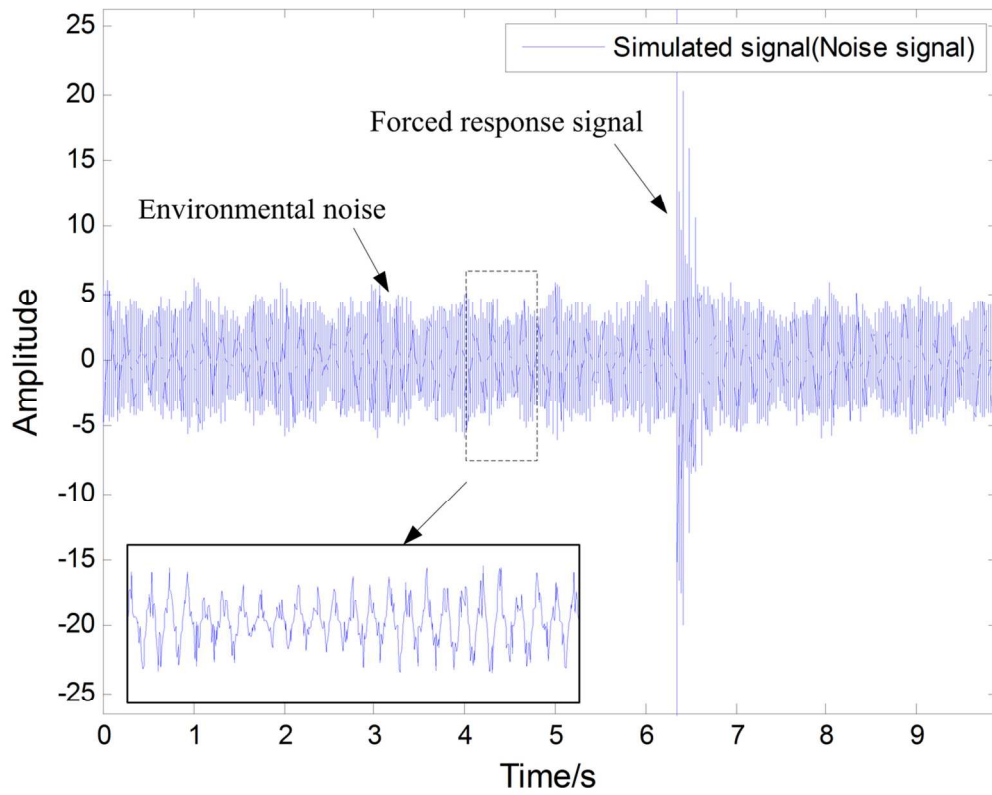
review

1
2
3
4
5
6
7
8
9
10
11
12
13
14
15
16
17
18
19
20
21
22
23
24
25
26
27
28
29
30
31
32
33
34
35
36
37
38
39
40
41
42
43
44
45
46
47
48
49
50
51
52
53
54
55
56
57
58
59
60

1
2
3
4
5
6
7
8
9
10
11
12
13
14
15
16
17
18
19
20
21
22
23
24
25
26
27
28
29
30
31
32
33
34
35
36
37
38
39
40
41
42
43
44
45
46
47
48
49
50
51
52
53
54
55
56
57
58
59
60

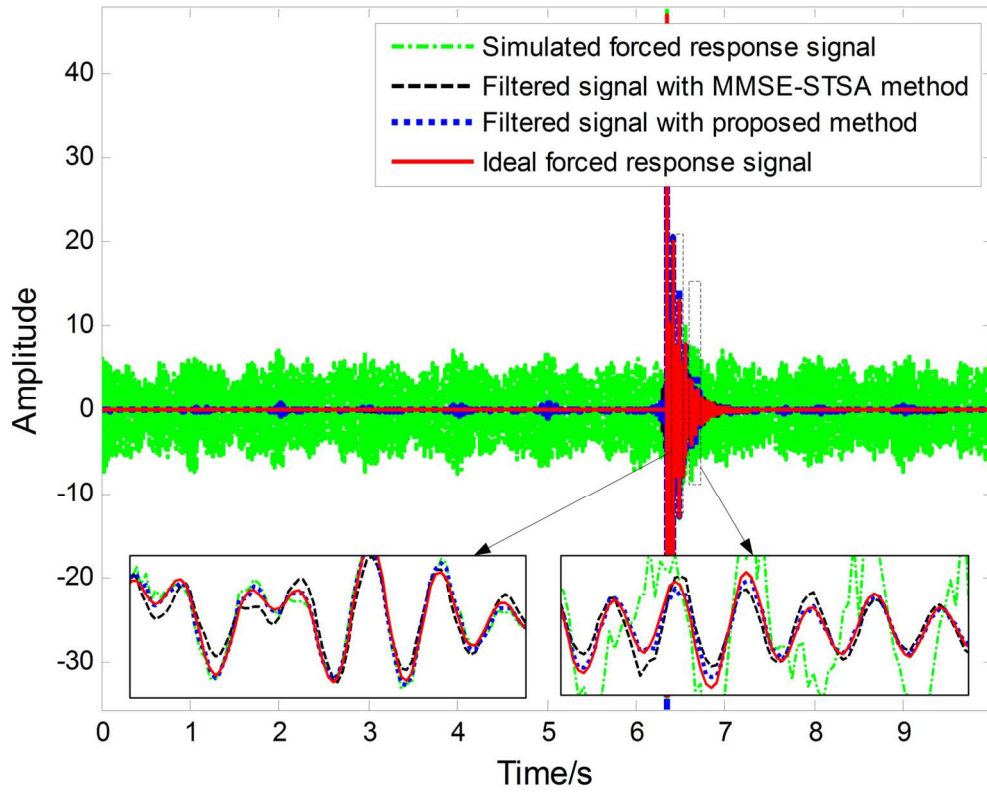


101x102mm (300 x 300 DPI)

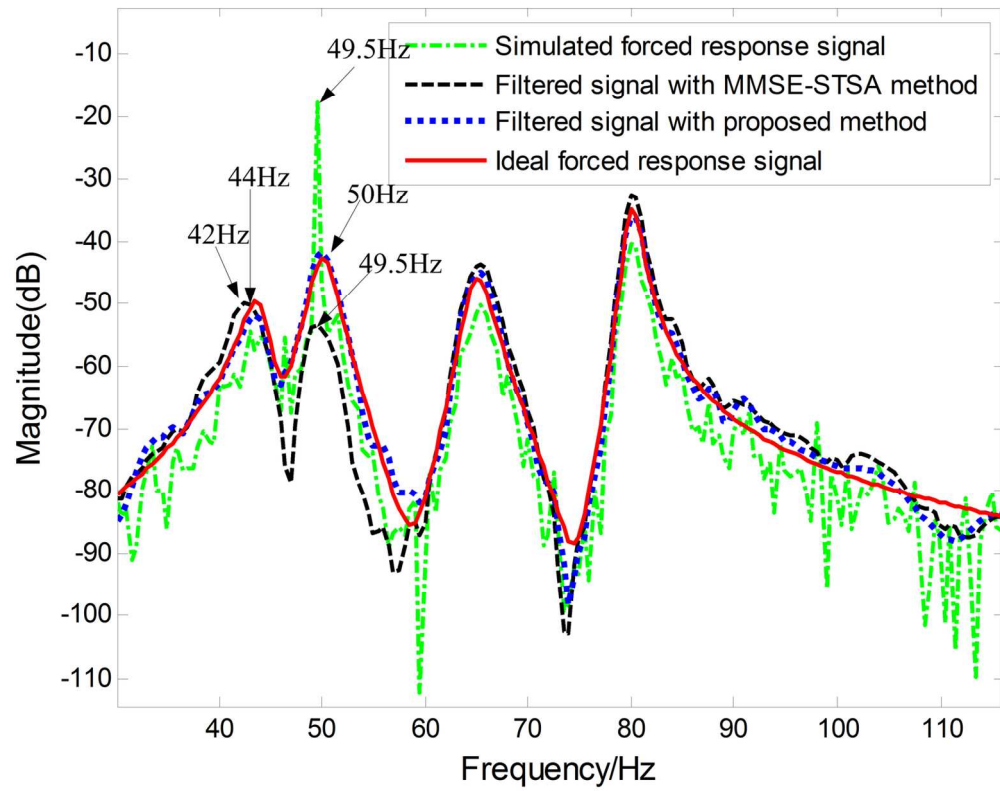


112x89mm (300 x 300 DPI)

1
2
3
4
5
6
7
8
9
10
11
12
13
14
15
16
17
18
19
20
21
22
23
24
25
26
27
28
29
30
31
32
33
34
35
36
37
38
39
40
41
42
43
44
45
46
47
48
49
50
51
52
53
54
55
56
57
58
59
60



135x107mm (300 x 300 DPI)

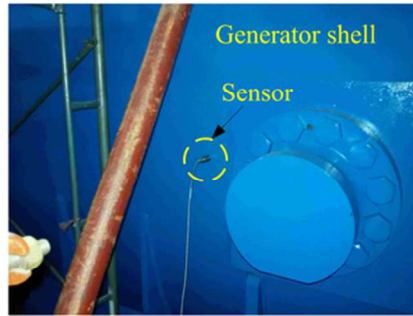


137x108mm (300 x 300 DPI)

1
2
3
4
5
6
7
8
9
10
11
12
13
14
15
16
17
18
19
20
21
22
23
24
25
26
27
28
29
30
31
32
33
34
35
36
37
38
39
40
41
42
43
44
45
46
47
48
49
50
51
52
53
54
55
56
57
58
59
60



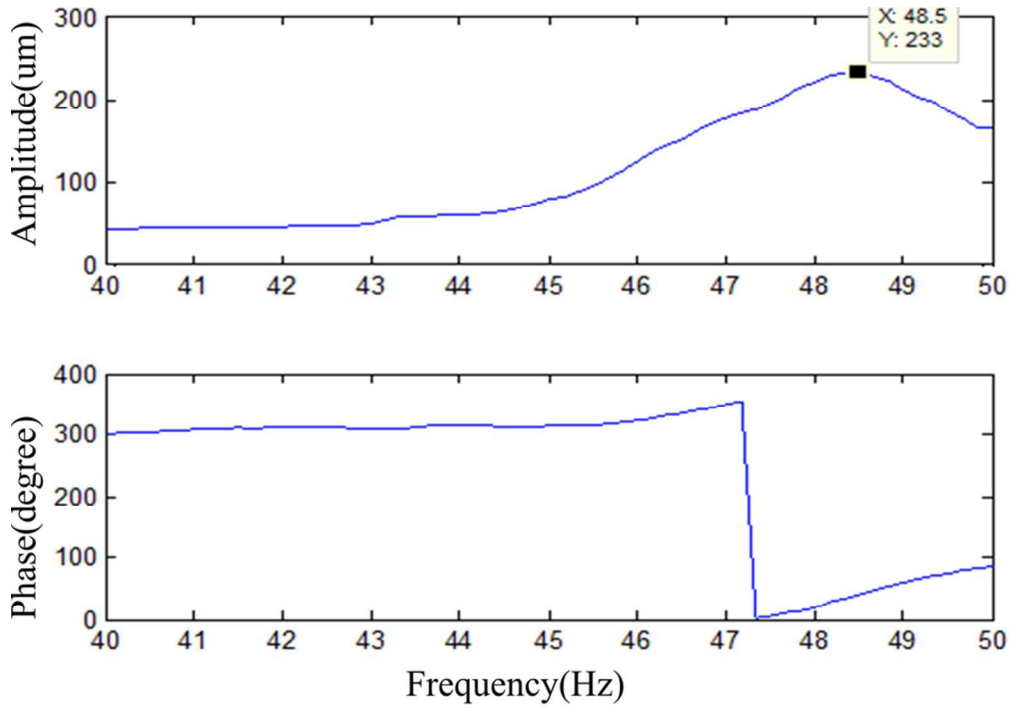
(a)



(b)

66x23mm (300 x 300 DPI)

Peer Review

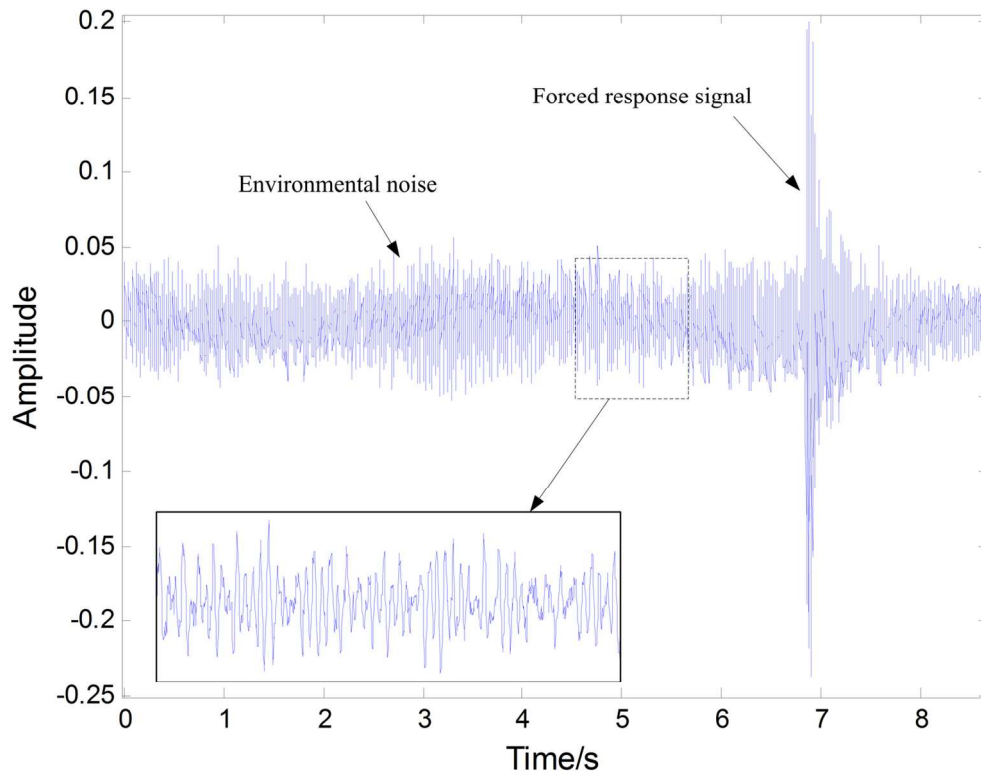


81x57mm (300 x 300 DPI)

Review

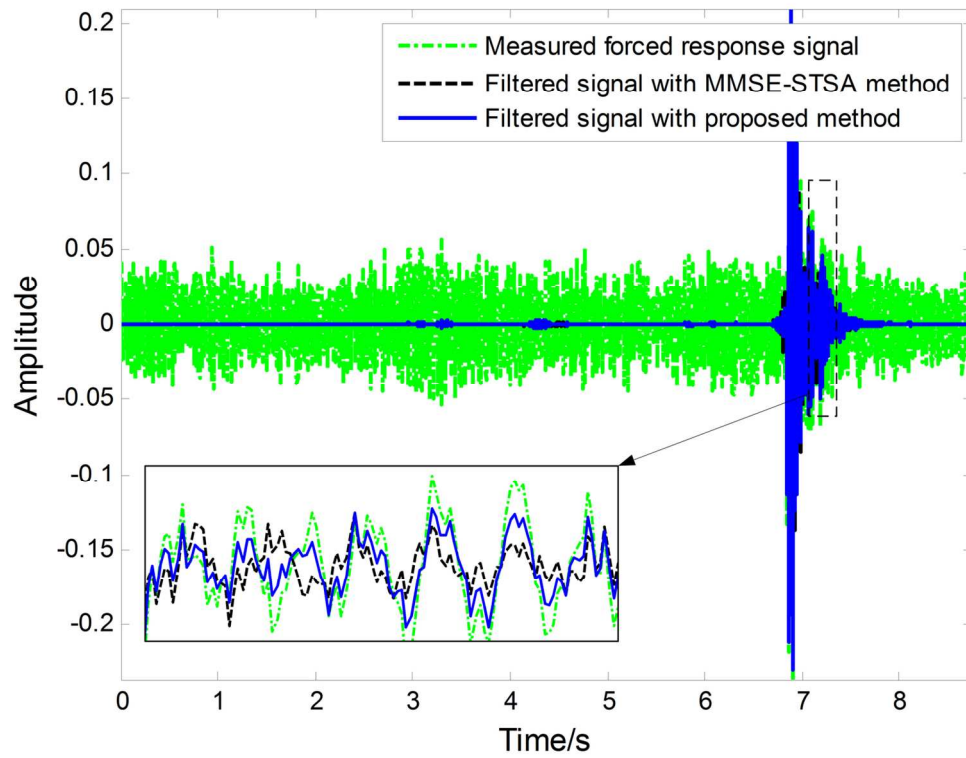
1
2
3
4
5
6
7
8
9
10
11
12
13
14
15
16
17
18
19
20
21
22
23
24
25
26
27
28
29
30
31
32
33
34
35
36
37
38
39
40
41
42
43
44
45
46
47
48
49
50
51
52
53
54
55
56
57
58
59
60

1
2
3
4
5
6
7
8
9
10
11
12
13
14
15
16
17
18
19
20
21
22
23
24
25
26
27
28
29
30
31
32
33
34
35
36
37
38
39
40
41
42
43
44
45
46
47
48
49
50
51
52
53
54
55
56
57
58
59
60



137x106mm (300 x 300 DPI)

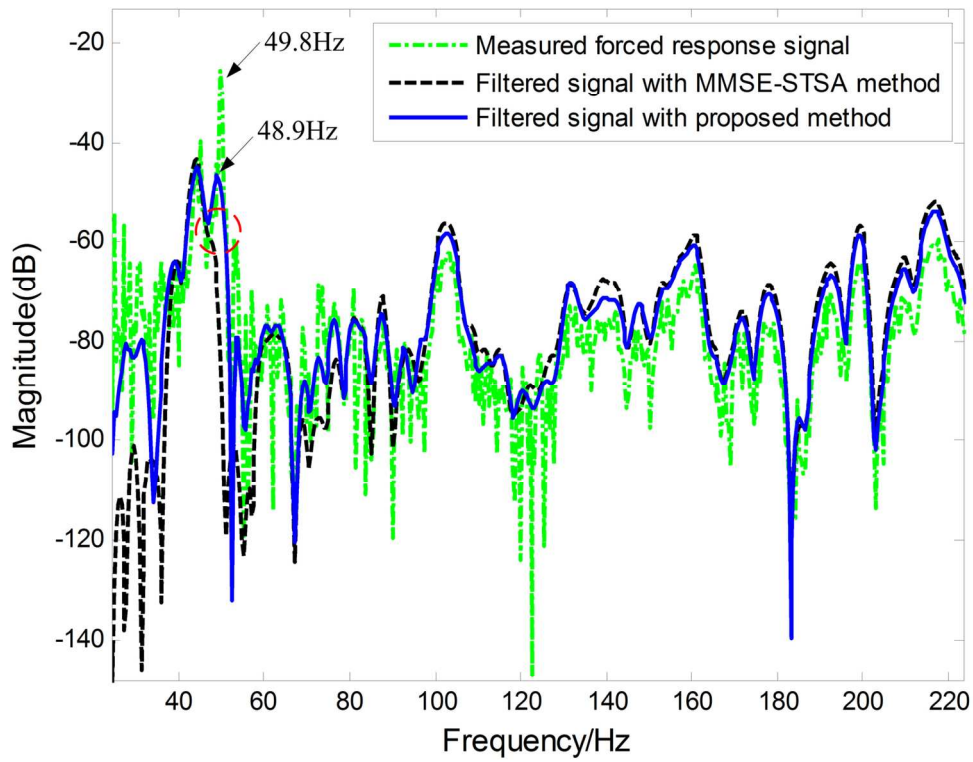
Review



135x105mm (300 x 300 DPI)

Review

1
2
3
4
5
6
7
8
9
10
11
12
13
14
15
16
17
18
19
20
21
22
23
24
25
26
27
28
29
30
31
32
33
34
35
36
37
38
39
40
41
42
43
44
45
46
47
48
49
50
51
52
53
54
55
56
57
58
59
60



139x107mm (300 x 300 DPI)

Review